MAGNETIC RESONANCE IN CHEMISTRY, VOL. 35, 877–882 (1997)

Novel Suppression of the Diagonal Signals in the NOESY Experiment

Matthias Baur and Horst Kessler*
Institut für Organische Chemie und Biochemie, TU München, Lichtenbergstrasse 4, D-85747 Garching, Germany

A pulse sequence is presented to record diagonal-peak-free NOESY spectra. The technique is based on the principle that those peaks which do not undergo chemical shift changes (via NOE) during the mixing time are suppressed. This is achieved by two jump-return units before and after the mixing time. A pulsed field gradient echo is used to obtain the suppression in one scan. The diagonal-peak-free NOESY spectrum exhibits a sine modulation of the cross-peak intensities caused by the jump-return selection. Unwanted zero quantum coherence (ZQC) is partially suppressed by the pulse sequence in each scan and residual ZQC is destroyed by *z*-filtering. The resulting spectra display a strong suppression of all diagonal peaks. Almost all residual ZQC artifact magnetization detected is absorptive in-phase. Hence almost all cross peaks of *J*-coupled protons are absorptive in-phase, reducing overlap. A practical application is presented, where additional experimental NOE data were obtained between amide protons of a cyclic peptide. © 1997 John Wiley & Sons, Ltd.

Magn. Reson. Chem. 35, 877–882 (1997) No. of Figures: 5 No. of Tables: 2 No. of References: 27

Keywords: NMR; ^{1}HNMR; peptides; NOESY; gradient echo; diagonal suppression; ZQC suppression

Received 12 May 1997; revised 27 June 1997; accepted 27 June 1997

INTRODUCTION

Structure determination of biopolymers mainly uses NOE-derived proton–proton distances obtained from multi-dimensional NOE spectroscopy.[1–5] The quality of the 3D structures strongly depends on the number and accuracy of well assigned NOE cross peaks. In peptides[6] especially, there is often an insufficient number of constraints leading to wrong, biased or ambiguous conformations. Here we present a new technique to suppress diagonal signals in NOESY spectra which enabled us to obtain additional cross peaks between amide protons suitable for structure refinement.

Two different approaches have been used so far to suppress diagonal peaks of NOESY spectra. The first group of efforts uses difference spectroscopy to subtract data representing the auto-signals from the normal NOESY spectrum.[7–9] As different pulse sequences are used to record the two data sets, these techniques require a high degree of fine tuning, and usually result in incomplete cancellation of the auto-peaks. The second group relies on folding techniques of the SECSY-type.[10,11] These experiments display a satisfactory suppression of auto-signals through phase cycling and co-addition. Here we present a technique that uses two jump-return units and pulsed field gradients as in the stimulated echo[12] and GOESY[13] experiments to suppress the diagonal peaks.

Correspondence to: H. Kessler. *E-mail*: kessler@artus.org.chemie.tu-muenchen.de

Contract grant sponsor: Deutsche Forschungsgemeinschaft.
Contract grant sponsor: Fonds der Chemischen Industrie.

EXPERIMENTAL

Figure 1(a) shows the pulse sequence for the diagonal-peak-free NOESY experiment. A stimulated echo[12] step is at the center a′–d′ of the experiment. The echo of auto-magnetization appears perpendicular to the direction of the 90° pulse applied at d (echo direction). The first pulse of the *z*-filter d′–f is phased to keep this echoed magnetization in coherence and this magnetization is subsequently destroyed by the spoil gradient G_{10}. The periods used for gradient encoding and decoding (called Δ_{JR}) simultaneously serve to separate the resonances based on their resonance frequency. Only magnetization that evolves during the second delay Δ_{JR} with a different resonance frequency than during the first delay Δ_{JR} will have a non-echo component, and will pass through the sequence, reminiscent of the jump-return experiment.[14,15] The cross peaks appear at the same positions as in the original NOESY spectra, but their intensities are modulated with a sheared sinusoidal profile with zero intensity at the diagonal. Neglecting coupling during the delays Δ_{JR}, the intensity of the cross peak $I \rightarrow S$ (proton I evolved during the indirect period t_1 and proton S evolved during the acquisition) is given by:

$$Int_{I\rightarrow S} = Int_{NOE}(\tfrac{1}{2})\sin[(\Omega_S - \Omega_I)\Delta_{JR}] \quad (1)$$

where Int_{NOE} indicates the intensity of the cross peak when using the original NOESY sequence and Ω_S and Ω_I indicate the resonance frequencies in the rotating frame of protons S and I, respectively. Equation (1) shows that the symmetrical cross peaks $I \rightarrow S$ and $S \rightarrow I$ carry opposite sign. The pulse sequence suppresses auto-magnetization and zero quantum coherence (ZQC)

CCC 0749–1581/97/120877–06 $17.50

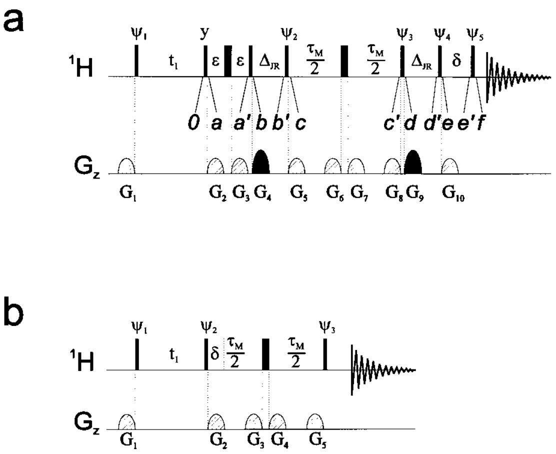

Figure 1. (a) Diagonal-peak-free NOESY and (b) z-filtered NOESY experiment[17] used to investigate compound **1** dissolved in DMSO-d_6. (a) Diagonal-peak-free NOESY: Quadrature detection in t_1 was performed according to the STATES-TPPI[26] protocol incrementing the phase of ψ_1. The phase cycling was $\psi_1 = y$; $\psi_2 = 8x, 8(-x)$; $\psi_3 = x, y, -x, -y$; $\psi_4 = y, -x, -y, x, -y, x, y, -x$; $\psi_5 = y, -x, -y, x$; Acq $= R, (-R)$; $R = x, y, -x, -y, -x, -y, x, y$. Pulses where no phase is given were applied along the x-axis. After completion of the phase cycle the delay δ was incremented and the phase cycle was restarted. Eleven increments from 0 to 6000 μs in equidistant steps of 600 μs were used.[23,24] Optionally, random variation of δ can be used (see Fig. 5). Pulsed field gradients (PFGs) in black produce a stimulated echo, whereas hatched PFGs serve as spoil gradients. PFGs G_6 and G_8 suppress artifact magnetization produced by T_1 relaxation.[27] PFG strengths were $G_1 = 5\%$, $G_2 = 25\%$, $G_3 = 6\%$, $G_4 = 60\%$, $G_5 = 34\%$, $G_6 = 12\%$, $G_7 = 4\%$, $G_8 = 5\%$, $G_9 = 60\%$ and $G_{10} = 12\%$, where 100% equals approximately 70 G cm^{-1}. PFGs had a sine-bell shape with a duration of 400 μs followed by a 400 μs recovery delay. Delays were $\varepsilon = 1.4$ ms, $\Delta_{JR} = 0.8$ ms and $\tau_M = 200$ ms. The recycle delay was 1.6 s, including the duration of acquisition. The r.f. power was 25 kHz for the ^{1}H hard pulse. (b) z-filtered NOESY: the acquisition followed the same procedure as for the diagonal-free NOESY. Phase cycling was $\psi_1 = y$; $\psi_2 = 4(y), 4(-y)$; $\psi_3 = x, y, -x, -y$; Acq $= x, y, -x, -y, -x, -y, x, y$. PFG strengths were $G_1 = 5\%$, $G_2 = 40\%$, $G_3 = 20\%$, $G_4 = 8\%$ and $G_5 = 4\%$. All other parameters were as described under (a).

in one scan. Residual ZQC is suppressed by varying the length of the z-filter d′–f.[16,17]

Owing to the single-scan gradient suppression, a high receiver gain is allowed. Typically 4 bits of dynamic resolution is won. Owing to the action of gradients G_4 and G_9, the sensitivity of the experiment is reduced to 50% of the original NOESY experiment [see Eqn (1)]. In addition, the sinusoidal modulation reduces the signal-to-noise ratio (S/N) of every individual peak, since the signal is reduced while the noise is unaffected. These reductions in S/N are partially compensated, since t_1 noise does not arise and hence the artifact level is considerably lowered.

The pathway of the desired single-quantum magnetization is described as follows. After initial excitation and evolution of proton magnetization the z-filter extending between times 0–b selects one transverse component of the magnetization. This is required for amplitude modulated quadrature detection. During the subsequent first jump-return delay Δ_{JR} the gradient G_4 labels the coherence of a particular proton I which will be later refocused by the gradient G_9 in the second jump-return delay. The coherence is then rotated into the z direction at time b′. During the mixing period c–c′ NOE transfer takes place. At c′ the magnetization is rotated back into the transverse plane and coherence is refocussed. At the end of the second delay Δ_{JR} (time d′) the auto-magnetization of proton I is aligned perpendicular to the direction of the 90° pulse applied at d (echo direction). Magnetization of a proton S which was transferred via NOE from proton I during the mixing time rotates to an angle $\Omega_S \Delta_{JR}$ during the second delay Δ_{JR}, rather than the angle $\Omega_I \Delta_{JR}$ covered by the same magnetization that remained on proton I. Therefore, this magnetization is not refocused along the echo direction, but rather falls ahead of or behind the echo direction, depending on whether the resonance frequency of S is higher or lower than the resonance frequency of I. For small differences in resonance frequency ($[\Omega_S - \Omega_I]\Delta_{JR} < \pi/2$) the angle between magnetization and echo direction increases with longer Δ_{JR}. The magnetization component of proton S perpendicular to the echo direction at time d′ is

$$M_S^{\perp} = M_{I \rightarrow S} \sin[(\Omega_S - \Omega_I)\Delta_{JR}] \tag{2}$$

where $M_{I \rightarrow S}$ denotes the amount of magnetization transferred via NOE from proton I to proton S during the mixing time. The first pulse of the final z-filter d′–f is phased to keep the echo of the auto-magnetization (proton I) in coherence. Subsequently this magnetization is destroyed by the spoil gradient G_{10}. Only the magnetization perpendicular to this orientation is finally detected. Therefore, the auto-peaks of all protons are eliminated and the intensity of cross peaks is modulated according to Eqn (1).

Suppression of magnetization stemming from zero-quantum coherence

Magnetization stemming from ZQC and passing the diagonal-peak-free NOESY sequence produces antiphase artifact peaks that mar the diagonal and taint the volumes of cross peaks of J-coupled protons. In addition, depending on the choice of the delay Δ_{JR}, weak in-phase ZQC-derived peaks are created on the diagonal or as cross peaks for J-coupled protons. Therefore, the experiment was optimized to suppress ZQC and ZQC-derived magnetization. The sequence in itself suppresses ZQC partially in each scan. Table 1 shows that for AX spin systems ZQC is *completely* dephased by pulsed field gradient action in one scan (any coupling during the delays Δ_{JR} is neglected). Residual ZQC is suppressed by varying the length of the z-filter d′–f.[16,17] ZQC-derived in-phase magnetization is avoided by proper choice of the delay Δ_{JR}. Proper values for peptides are $\Delta_{JR} < 800$ μs (see below).

RESULTS AND DISCUSSION

The diagonal-peak-free NOESY experiment [Fig. 1(a)] was applied to the cyclic pentapeptide cyclo(–D-Arg–Gly–D-Asp–Phe–D-Val–)[18] (**1**) and a sugar derivative (**2**).[19] As shown by the ^3J(H,H) coupling constants, ^{13}C chemical shifts and NOE restraints, **2** preferentially assumes the unusual $^1C_4$ conformation in chloroform.[20]

Table 1. ZQC derived magnetization in product operator description[25] at times 0–f in the diagonal-peak-free NOESY sequence of Fig. 1(a)[a]

At	Product operator
0	$\boldsymbol{2I_yS_z} - 2I_xS_z$
a	$2I_yS_x = \underbrace{(I_yS_x + I_xS_y)}_{\text{DQC}} + \underbrace{(\boldsymbol{I_yS_x - I_xS_y})}_{\text{ZQC}}$
a′	$\boldsymbol{I_xS_y - I_yS_x}$
b	$\boldsymbol{I_xS_z - I_zS_x}$
b′	$[\boldsymbol{S_zI_{x(\cos I):g}} + S_zI_{y(\sin I):g}] - [\boldsymbol{I_zS_{x(\cos S):g}} + I_zS_{y(\sin S):g}]$
c	$-S_yI_{x(\cos I):g} + I_yS_{x(\cos S):g} = -(\tfrac{1}{2})[\boldsymbol{S_yI_{x(\cos I):g} - S_{x(\cos I):g}I_y}] + (\tfrac{1}{2})[\boldsymbol{I_yS_{x(\cos S):g} - I_{x(\cos S):g}S_y}] + \text{DQC}$
c′	$(\tfrac{1}{2})[\boldsymbol{S_yI_{x(\cos I):g} - S_{x(\cos I):g}I_y}] - (\tfrac{1}{2})[\boldsymbol{I_yS_{x(\cos S):g} - I_{x(\cos S):g}S_y}]$
d	$(\tfrac{1}{2})[\boldsymbol{S_zI_{x(\cos I):g} - S_{x(\cos I):g}I_z}] - (\tfrac{1}{2})[\boldsymbol{I_zS_{x(\cos S):g} - I_{x(\cos S):g}S_z}]$
d′	$(\tfrac{1}{4})(S_zI_x - \{S_xI_z\cos[(\Omega_I - \Omega_S)\Delta_{JR}] - \boldsymbol{S_yI_z}\,\mathbf{sin}[(\boldsymbol{\Omega_I - \Omega_S})\boldsymbol{\Delta_{JR}}]\}) - (\tfrac{1}{4})(I_zS_x - \{I_xS_z\cos[(\Omega_I - \Omega_S)\Delta_{JR}] + \boldsymbol{I_yS_z}\,\mathbf{sin}[(\boldsymbol{\Omega_I - \Omega_S})\boldsymbol{\Delta_{JR}}]\})$
e	$(\tfrac{1}{4})\underbrace{(S_yI_x + I_yS_x)}_{\text{DQC}}\sin[(\Omega_I - \Omega_S)\Delta_{JR}]$
e′	$\mathbf{0}$

[a] An AX spin system is assumed. Coupling during the delays $\boldsymbol{\Delta_{JR}}$ and relaxation is neglected. Product operators that will be destroyed by the next spoil-gradient and who are dropped from the analysis are in normal type. The extensions of the index $(\cos I):g$ and $(\sin I):g$ are shorthand for amplitude modulations that result from the added effects of spin evolution during time $\boldsymbol{\Delta_{JR}}$ and the action of the gradient G_4 according to

$$I_x \xrightarrow{\Omega_I \Delta_{JR} I_z} I_x\cos(\Omega_I\Delta_{JR}) + I_y\sin(\Omega_I\Delta_{JR}) \xrightarrow{G_4}$$

$$I_x\cos[\Omega_I\Delta_{JR} + \phi_{\text{coil}}(z)] + I_y\sin[\Omega_I\Delta_{JR} + \phi_{\text{coil}}(z)] = I_{x(\cos I):g} + I_{y(\sin I):g}$$

where $\boldsymbol{\Omega_I}$ denotes the resonance frequency of proton I and $\boldsymbol{\phi}_{\text{coil}}(z)$ the phase added by gradient G_4 when twisting the transverse magnetization into a coil along the z-direction.

Compound 1 was dissolved in DMSO-d_6 (concentration 25 mM) and measured at 600 MHz on a Bruker AMX600 spectrometer at 300 K. The NOE build-up is negative. In Fig. 2 the amide proton region of the diagonal-peak-free NOESY spectrum is compared with the same region of a z-filtered NOESY spectrum. In the diagonal-peak-free NOESY experiment the delay $\Delta_{JR} = 800$ µs was used. The corresponding modulation profile is shown in Fig. 3. The suppression of the diagonal peaks can be seen from a representative row of each spectrum at the resonance frequency of D-Arg^1 H^N (Fig. 4). It is obvious that only in the diagonal-peak-free NOESY spectrum is the D-Arg^1 H^N → D-Val^5 H^N cross peak detached from the diagonal. The other cross peaks near the strong diagonal in the z-filtered NOESY spectrum appear more accurately in the diagonal-peak-free

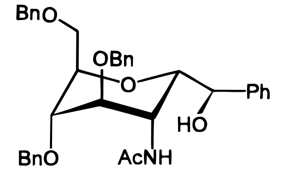

2

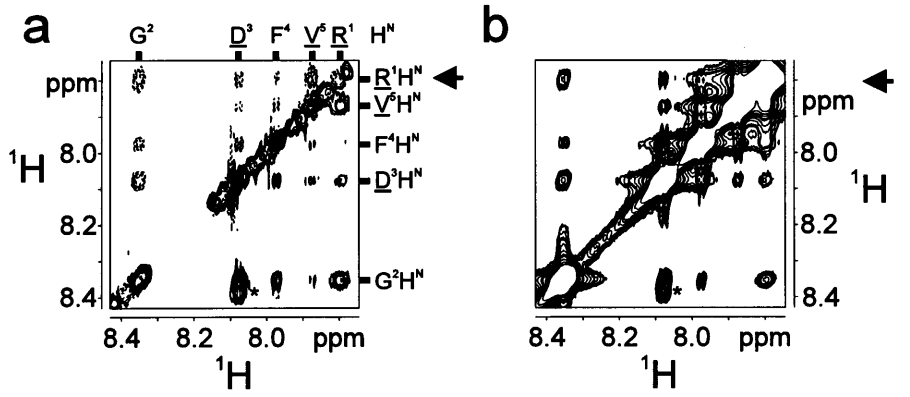

Figure 2. Details from (a) the diagonal-peak-free NOESY and (b) the z-filtered NOESY spectra of compound **1**. The recordings followed the procedures described in Fig. 1. The diagonal-peak-free NOESY was recorded with a receiver gain 16 times higher than for the z-filtered NOESY. Both spectra were recorded as 8192 × 256 real points in the acquisition (Acq) and t_1 domain, respectively. The spectral widths were 7353 × 1802 Hz (Acq × t_1). The measurement time was 12 h each. Both data sets were processed to a matrix of 4096 × 256 real points after application of a 90° shifted sine-bell window function and subsequent zero filling. In the case of the z-filtered NOESY a baseline correction by subtracting of a fifth-order polynomial from the spectral data along the Acq domain was done, followed by the same procedure along the t_1 domain. The spectra are displayed slightly above the noise level in the case of the diagonal-peak-free NOESY and slightly above the level of t_1 artifacts in the case of the z-filtered NOESY. An asterisk indicates cross peaks folded into the zoomed region.

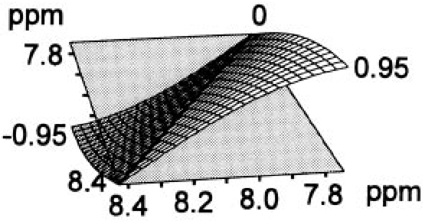

Figure 3. Sinusoidal modulation profile of the intensity in the diagonal-peak-free NOESY spectrum [Fig. 2(a)]. The period of modulation is 2.08 ppm.

NOESY spectrum. Respective cross peaks were integrated on both sides of the diagonal and averaged, taking into account the opposite signs. The average volumes, Int_{noD}, have to be corrected for the modulation according to

$$Int_{\mathrm{corr}} = Int_{\mathrm{noD}}/\sin(2\pi\ \Delta\Omega\ \Delta_{\mathrm{JR}}) \qquad (3)$$

where $\Delta\Omega = \Omega_{\mathrm{S}} - \Omega_{\mathrm{I}}$ denotes the chemical shift separation of the correlated protons in Hz. Subsequently the corrected intensities Int_{corr} were transformed into distances using the isolated two-spin approximation (ISPA).[21] The cross-peak intensities of the geminal protons D-Asp^3 H$^{\beta}$–D-Asp^3 H$^{\beta'}$ and D-Arg^1 H$^{\beta}$–Arg^1 H$^{\beta'}$ were used as a reference. The fact that the corrected intensities Int_{corr} of the cross peaks of the two geminal proton pairs, that have different chemical shift separations ($\Delta\Omega = 0.23$ ppm and $\Delta\Omega' = 0.30$ ppm) are in close agreement indicated that contributions by artifacts are negligible. For comparison, corresponding signals in the z-filtered NOESY spectrum were evaluated. The cross peaks were integrated using footprints similar to those employed for the diagonal-peak-free NOESY. Then the averaged intensities (below and above the diagonal) were translated into distances using the ISPA. No effort was made to correct for the residual intensity of the diagonal peak for peaks on the flank of the diagonal. All distances are given in Table 2.

It is obvious that distances derived from signals far away from the diagonal are identical in both spectra to within 10%. However, considerable deviations can be found for peaks close to the diagonal. The integrals of these peaks (in bold type in Table 2) appear too large in the z-filtered NOESY spectrum. Therefore, it seems that an approach of extracting individual slices, subtracting the diagonal-peak intensity and integrating the cross peaks should give improved results from the z-filtered NOESY. However, such an approach does not address artifact intensity from t_1 noise. Given the small intensity of some cross peaks (where $r > 350$ pm), this seems very worrisome. The more reliable distances from the diagonal-peak-free NOESY spectrum have been used for a structure refinement of **1** using an ensemble approach.[22]

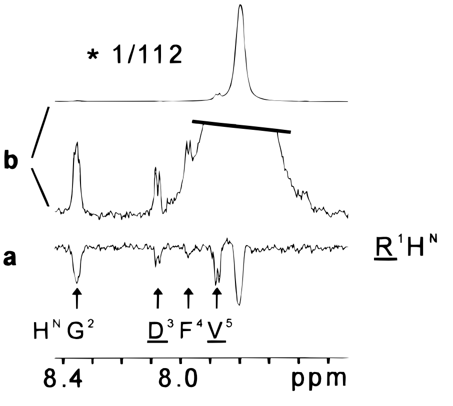

Figure 4. Rows extracted from the spectra in (a) Fig. 2(a) and (b) Fig. 2(b) at the chemical shift of D-Arg^1 H^N in the t_1 domain (indicated by an arrow in Fig. 2). Both rows are plotted at the same level. The theoretical and experimental S/N reductions of (a) vs (b) for the peak D-Arg^1 H$^N \rightarrow$ Gly^2 H^N are $0.50 \sin(1.05\ \pi/2) \approx 0.50$ and 0.5, respectively. The theoretical and experimental S/N reductions for the peak D-Arg^1 H$^N \rightarrow$ Phe^4 H^N are $0.50 \sin(0.33\ \pi/2) \approx 0.25$ and 0.2, respectively.

Table 2. Proton distances in compound 1 obtained from the diagonal-peak-free NOESY (r_{noD}) and the *z*-filtered NOESY (r_{NOE}) spectra using the ISPA[21] approach[a]

H$_1$	H$_2$	ΔΩ (ppm)	r_{noD} (pm)	r_{NOE} (pm)
Gly^2 H^N	D-Arg^1 H^N	0.56	305	317
Gly^2 H^N	Phe^4 H^N	0.38	348	380
Gly^2 H^N	D-Asp^3 H^N	0.28	286	290
D-Asp^3 H^N	D-Arg^1 H^N	0.28	353	361
D-Asp^3 H^N	D-Val^5 H^N	0.21	369	363
D-Asp^3 H^N	Phe^4 H^N	0.10	**308**	263
Phe^4 H^N	D-Arg^1 H^N	0.18	**389**	291
Phe^4 H^N	D-Val^5 H^N	0.10	**343**	259
D-Val^5 H^N	D-Arg^1 H^N	0.08	**255**	199
D-Arg^1 H$^{\beta}$	D-Arg^1 H$^{\beta'}$	0.23	183	182
D-Arg^1 H$^{\delta}$	D-Arg^1 H$^{\beta'}$	1.59	281	292
D-Asp^3 H$^{\beta}$	D-Asp^3 H$^{\beta'}$	0.30	178[b]	178[b]

[a] The diagonal-peak-free NOESY intensities were corrected for the modulation according to Eqn (3) prior to transformation. Distances, where major deviations between the two experiments are observed, are in bold type.

[b] cross-peak used for calibration.

To investigate the effect of J-couplings on the quality of a diagonal-peak-free NOESY spectrum, the C-glycosidic derivative of N-acetylglucosamine **2** in $CDCl_3$ (concentration 60 mM) was measured at 600 MHz and 300 K on a Bruker AMX600 spectrometer. As the NOE build-up is very weak (positive sign) and the decay of transverse magnetization is slow, J-artifact peaks are relatively strong. Figure 5(a) shows a detail of the diagonal-peak-free NOESY spectrum, containing the cross peaks of the geminal protons of two benzyl protection groups. The same detail of a z-filtered NOESY spectrum is displayed in Fig.5(b). The in-phase signals for cross peaks of J-coupled protons observed in Fig. 5(a), are typical for the diagonal-peak-free NOESY. Suppression of the ZQC artifact anti-phase pattern renders the small cross peak from an impurity of the sample at 4.48 ppm–4.66 ppm invisible in Fig. 5(a). As both spectra were measured with the same z-filter variation scheme, the absence of dispersive contributions in the diagonal-peak-free NOESY spectrum compared with the z-filtered NOESY spectrum demonstrates the ZQC suppression afforded by the sequence according to Table 1. Distances were evaluated from the diagonal-peak-free NOESY spectrum using the same procedure as for **1**. The ISPA calibration was performed by aligning the experimental distances for various cross peaks of non-J-coupled protons with

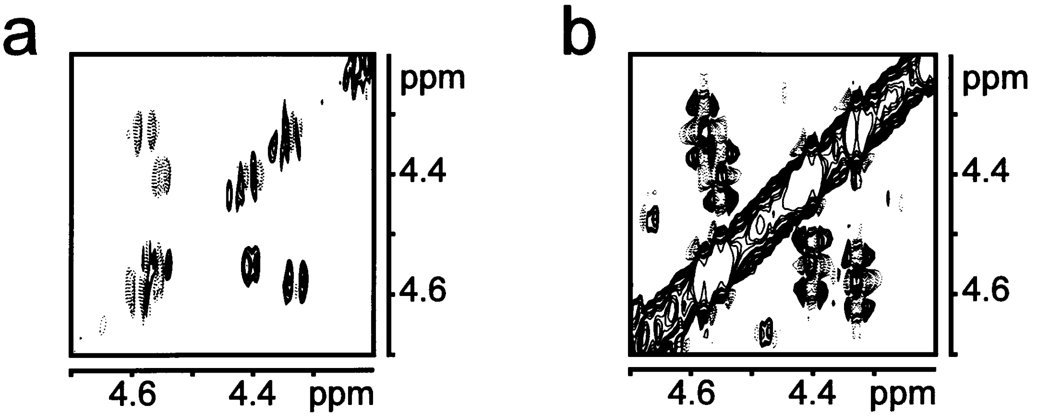

Figure 5. Details from spectra recorded with (a) the diagonal-peak-free NOESY and (b) the *z*-filtered NOESY on compound **2**. The recordings followed the procedures described in Fig. 1. However, the *z*-filter width *δ* was randomly varied from scan to scan between 6 and 10 ms[23] and Δ_{JR} was 600 μs. Both spectra were recorded with 4096 real points in the acquisition (Acq) domain and 512 real points in the t_1 domain. The spectral width was 6667 Hz in both dimensions. The measurement time was 4 h each. Both data sets were processed to a matrix of 4096 × 1024 real points after application of a 90° shifted sine-bell window function and subsequent zero filling. In the case of the *z*-filtered NOESY a fifth-order polynomial was subtracted from the frequency domain data to remove noise ridges in the Acq and t_1 dimensions. The spectra are displayed at approximately equal levels. The cross peak at 4.48–4.66 ppm and its partner on the other side of the diagonal in the right-hand spectrum have nearly zero intensity and are anti-phase ZQC artifacts of an impurity of the sample.

the distances observed in the $^1C_4$ conformation. For comparison, the corresponding distances in the *z*-filtered NOESY spectrum were evaluated, using integration limits that extend around the entire pattern of cross peaks of *J*-coupled protons. Diagonal-peak-free NOESY distances for the geminal protons shown in Fig. 5 were 187 pm (cross peak closer to the diagonal) and 196 pm and the *z*-filtered NOESY distances were 212 and 189 pm. Optimization of the *z*-filtered NOESY for geminal protons (*z*-filtering with an 11-step cycle by incrementing the filter width, *δ*, from 0 to 6000 μs in equidistant steps of 600 μs)[23,24] resulted in very similar peak patterns but in improved distances of 192 and 187 pm. Inspection of the distances from the diagonal-peak-free NOESY spectrum shows that the volumes for cross peaks of *strongly J*-coupled protons contain artifact contributions. One such contribution is caused by the mis-setting of the proton pulse. Since the diagonal-peak-free NOESY contains more pulses than the *z*-filtered NOESY (nine in the former, four in the latter), this contribution is stronger in a diagonal-peak-free NOESY. An additional contribution is produced by coupling during the Δ_{JR} periods due to transfers of the following type: ZQC after first 90° pulse following the evolution time t_1 (time *a*) → anti-phase at beginning of second delay Δ_{JR} → SQC at end of second delay Δ_{JR} → SQC detected. With the proper choice of Δ_{JR} (see below) this contribution is usually smaller than the contribution from proton pulse mis-setting. Inspection of the distances from the z-filtered NOESY spectrum shows that the cross peaks of strongly *J*-coupled protons also suffer artifact contributions. These artifacts are mainly due to mis-setting of the proton pulse and similar reasons, that weigh in strongly since the NOE in **2** is very weak. In summary, the additional measures in the diagonal-peak-free NOESY compensate to a large extent for additional sources of ZQC artifact magnetization and the sequence is only slightly inferior to an optimized *z*-filtered NOESY regarding the quality of distances from cross peaks of strongly *J*-coupled protons.

To determine the proper choice of Δ_{JR} we recorded a series of diagonal-peak-free NOESY spectra varying the delay Δ_{JR}. This series showed that the residual artifact contribution in the cross peaks of strongly *J*-coupled protons grows rapidly with increasing sizes of Δ_{JR} and *J*-coupling constant, while decreasing rapidly with growing chemical shift separation $\Delta\Omega$ of the correlated protons. Therefore, the use of a small Δ_{JR} delay (400 μs $< \Delta_{JR} <$ 800 μs) is recommended. In addition, based on these results an ISPA calibration using the intensity $Int_{\rm corr}$ of a geminal cross peak is accurate, if the same intensity $Int_{\rm corr}$ is obtained for another geminal cross peak with different chemical shift separation $\Delta\Omega'$.

CONCLUSION

We have described a pulse sequence to record diagonal-peak-free NOESY spectra. The experiment is based on the principle that all peaks which do not undergo chemical shift changes (via NOE) during the mixing time are suppressed. This is achieved by two jump-return units before and after the mixing time. A pulsed field gradient homonuclear echo is used to obtain the suppression in one scan. The spectra have the usual appearance of NOESY spectra, but the intensity is modulated by a sheared sinusoidal profile with zero intensity at the diagonal caused by the jump-return selection. The sequence partially suppresses unwanted contributions of ZQC in each scan, and residual ZQC is destroyed by *z*-filtering. Owing to these measures, the sequence is only slightly inferior to an optimized *z*-filtered NOESY regarding quality of distances of *strongly J*-coupled peaks. The experimental spectra display a strong suppression of all diagonal peaks. In addition, most residual ZQC artifact magnetization detected is absorptive in-phase, reducing peak overlap. The new experiment was used successfully to obtain additional NOE derived distances between amide protons with small chemical shift separation, that could not be obtained from a normal NOESY.

Acknowledgements

This work was supported by the Deutsche Forschungsgemeinschaft and the Fonds der Chemischen Industrie. We thank R. Gschwind, M. Bachelin, M. Coles and G. Gemmecker (Technische Universität München) for helpful discussions. Many thanks go to M. Hoffmann and J. Wermuth (Technische Universität München) for supplying the samples.

REFERENCES

1. J. Jeener, B. H. Meier, P. Bachmann and R. R. Ernst, *J. Chem. Phys.* **71**, 4546 (1979).
2. A. Kumar, R. R. Ernst and K. Wüthrich, *Biochem. Biophys. Res. Commun.* **95**, 1 (1980).
3. K. Wüthrich, *NMR of Proteins and Nucleic Acids*, pp. 117–130. Wiley, New York (1986).
4. S. W. Fesik and E. R. P. Zuiderweg, *J. Magn. Reson.* **78**, 588 (1988).
5. L. E. Kay, G. M. Clore, A. Bax and A. M. Gronenborn, *Science*, **249**, 411 (1990).
6. H. Kessler, R. K. Konat and W. Schmitt, *in NMR in Drug Design*, edited by D. J. Craik, CRC Series in Analytical Biotechnology, pp. 215–244. CRC Press, Boca Raton, FL (1996).
7. G. Bodenhausen and R. R. Ernst, *Mol. Phys.* **47**, 319 (1982).
8. W. Denk, G. Wagner, M. Rance and K. Wüthrich, *J. Magn. Reson.* **62**, 350 (1985).
9. C. Dalvit, G. Bovermann and H. Widmer, *J. Magn. Reson.* **88**, 432 (1990).
10. K. Nagayama, Y. Kobayashi and Y. Kyogoku, *J. Magn. Reson.* **51**, 84 (1983).
11. G. S. Harbison, J. Feignon, D. J. Ruben, J. Herzfeld and R. G. Griffin, *J. A. Chem. Soc.* **107**, 5567 (1985).
12. J. E. Tanner, *J. Chem. Phys.* **52**, 2523 (1970).
13. J. Stonehouse, P. Adell, J. Keeler and A. J. Shaka, *J. Am. Chem. Soc.* **116**, 6037 (1994).
14. P. Plateau and M. Gueron, *J. Am. Chem. Soc.* **104**, 7310 (1982).
15. J. Stonehouse, G. L. Shaw and J. Keeler, *J. Biomol. NMR* **4**, 799 (1994).
16. S. Macura, Y. Huang, D. Suter and R. R. Ernst, *J. Magn. Reson.* **43**, 259 (1981).
17. M. Rance, G. Bodenhausen, G. Wagner, K. Wüthrich and R. R. Ernst, *J. Magn. Reson.* **62**, 497 (1985).
18. M. Gurrath, G. Müller, H. Kessler, M. Aumailley and R. Timpl, *Eur. J. Biochem.* **210**, 911 (1992).
19. M. Hoffmann and H. Kessler, *Tetrahedron Lett.* **35**, 6067 (1994).
20. M. Hoffmann, Thesis, Technical University of Munich (1996).
21. D. Neuhaus, M. Williamson, *The Nuclear Overhauser Effect in Structural and Conformational Analysis*. VCH, Weinheim (1989).
22. D. F. Mierke, M. Kurz and H. Kessler, *J. Am. Chem. Soc.* **116**, 1042 (1994).
23. S. Macura, Y. Huang, D. Suter and R. R. Ernst, *J. Magn. Reson.* **43**, 259 (1981).
24. M. Rance, G. Bodenhausen, G. Wagner, K. Wüthrich and R. R. Ernst, *J. Magn. Reson.* **62**, 497 (1985).
25. H. Kessler, M. Gehrke and C. Griesinger, *Angew. Chem., Int. Ed. Engl.* **27**, 490 (1988).
26. D. Marion, M. Ikura, R. Tschudin and A. Bax, *J. Magn. Reson.* **85**, 393 (1989).
27. J. V. Hines, S. M. Landry, G. Varani and I. Tinoco, *J. Am. Chem. Soc.* **116**, 5823 (1994).